Available online at www.sciencedirect.com

SCIENCE DIRECT®

Thermochimica Acta 431 (2005) 133–137

thermochimica acta

www.elsevier.com/locate/tca

Heat capacity and magnetic phase transition of two-dimensional metal-assembled complex, $K[\{Mn^{III}(3\text{-}MeOsalen)\}_2Fe^{III}(CN)_6]$☆

Yuji Miyazaki[a,*], Qi Wang[a,b], Qing-sen Yu[a,b], Tetsuya Matsumoto[a],
Hitoshi Miyasaka[c], Naohide Matsumoto[d], Michio Sorai[a]

[a] *Research Center for Molecular Thermodynamics, Graduate School of Science, Osaka University, Toyonaka, Osaka 560-0043, Japan*
[b] *Department of Chemistry, Zhejiang University, Hangzhou 310027, PR China*
[c] *Department of Chemistry, Graduate School of Science, Tokyo Metropolitan University, Minami-ohsawa 1-1, Hachioji, Tokyo 192-0397, Japan*
[d] *Department of Chemistry, Faculty of Science, Kumamoto University, 2-39-1 Kurokami, Kumamoto 860-8555, Japan*

Received 22 October 2004; received in revised form 26 November 2004; accepted 26 January 2005
Available online 25 February 2005

Abstract

Heat capacities of the two-dimensional metal-assembled complex, $K[\{Mn^{III}(3\text{-}MeOsalen)\}_2Fe^{III}(CN)_6]$ [3-MeOsalen = *N*,*N*′-ethylenebis(3-methoxysalicylideneaminato) dianion], were measured at the temperatures from 0.5 to 300 K by adiabatic calorimetry. An antiferromagnetic phase transition was observed at $T_N = 8.29$ K. Above T_N, a heat capacity tail arising from the short-range-order effect of the spins was found, which is characteristic of two-dimensional magnets. The magnetic enthalpy and entropy were evaluated to be $\Delta H = 373\ \mathrm{J\,mol^{-1}}$ and $\Delta S = 31.3\ \mathrm{J\,K^{-1}\,mol^{-1}}$, respectively. The experimental magnetic entropy is in good agreement with $\Delta S = R \ln (5 \times 5 \times 2)$ (=32.5 $\mathrm{J\,K^{-1}\,mol^{-1}}$; *R* being the gas constant), which is expected for the metal complex with two Mn(III) ions in high spin state (spin quantum number $S = 2$) and one Fe(III) ion in low spin state ($S = 1/2$). The spin wave analysis suggests that the complex shows three-dimensional antiferromagnetic order below T_N. The heat capacity tail above T_N was decreased by grinding and pressurizing the crystal. This mechanochemical effect would originate in the increase of lattice defects and imperfections in the crystal lattice, leading to decrease of the magnetic heat capacity and hence the magnetic enthalpy and entropy.
© 2005 Elsevier B.V. All rights reserved.

Keywords: Metal-assembled complex; Heat capacity; Magnetic phase transition; Mechanochemical effect

---

1. Introduction

Research and development on molecular magnetism have been advancing in the last decade [1–7]. Particularly, new types of metal complexes formed by assembling some kinds of metal complexes in a higher-order structure, the so-called “metal-assembled complexes”, have been attracting many researchers, because they may have the possibilities of formation of specific spatial, electronic, and magnetic structures, which are hardly realized in classical organic, inorganic, and metal complex systems.

Metal-assembled complexes of the type of $X_k[A(L)]_l[B(CN)_6]_m \cdot nS$ (X: monovalent nonmagnetic ion; A, B: di- or trivalent transition metal ions; L: organic ligand; S: solvate molecule; *k*, *l*, *m*, *n*: numbers of stoichiometry) can form various network structures depending on A, B, and L. Based on this strategy, many complexes have so far been synthesized and investigated [8–11].

The present metal-assembled complex, $K^+[\{Mn^{III}(3\text{-}MeOsalen)^{2-}\}_2Fe^{III}(CN^-)_6]$ [3-MeOsalen = *N*,*N*′-ethylenebis(3-methoxysalicylideneaminato) dianion, abbreviated as MnFe-mos; Fig. 1(a)], has been synthesized by reacting $[Mn(3\text{-}MeOsalen)(H_2O)]ClO_4$ and $K_3[Fe(CN)_6]$ [8,9]. This complex contains two high-spin trivalent Mn ions (spin quantum number $S = 2$) and one low-spin trivalent Fe ion ($S = 1/2$) per formula unit. X-ray structural analysis

---

☆ No. 89 from the Research Center for Molecular Thermodynamics.
* Corresponding author. Tel.: +81 6 6850 5524; fax: +81 6 6850 5526.
E-mail address: miyazaki@chem.sci.osaka-u.ac.jp (Y. Miyazaki).

0040-6031/$ – see front matter © 2005 Elsevier B.V. All rights reserved.
doi:10.1016/j.tca.2005.01.059

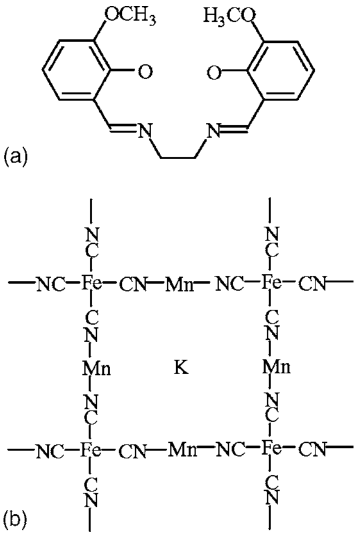

Fig. 1. (a) Molecular structure of 3-MeOsalen. (b) Schematic drawing of two-dimensional assembly of $[Mn(3\text{-}MeOsalen)]^+$ and $[Fe(CN)_6]^{3-}$ in the MnFe-mos crystal, where $[Mn(3\text{-}MeOsalen)]^+$ is simply expressed by Mn.

of $K[\{Mn(3\text{-}MeOsalen)\}_2Fe(CN)_6]\cdot 2DMF$ (DMF = *N*,*N*-dimethylformamide) crystal [8,9] revealed that this complex is crystallized in monoclinic system with the space group $P2_1/c$ and forms a two-dimensional network structure consisting of 2:1 of $[Mn(3\text{-}MeOsalen)]^+$ and $[Fe(CN)_6]^{3-}$ as illustrated in Fig. 1(b). Magnetic susceptibility measurement of a powder MnFe-mos sample [8,9] revealed that there is a ferromagnetic interaction through the Fe–CN–Mn bridge evidenced by a positive Weiss constant $\Theta = +6.8$ K. In field-cooled magnetization (FCM) measurement [9], magnetizations of both powder and crystalline MnFe-mos samples show sharp peaks at 9.2 K under 100 Oe of magnetic field, while those determined under 300 Oe have no peaks and remain constant after the abrupt increment at ca. 9 K, suggesting metamagnetism below the antiferromagnetic phase transition $T_N = 9.2$ K.

Heat capacity measurement is a powerful tool together with magnetic measurement for elucidation of magnetic properties of substances [12–16]. Especially, adiabatic calorimetry enables us to get information about precise magnetic phase transition temperature, heat capacity, and entropy. Moreover, analyses of magnetic heat capacity and entropy provide us with the insight into the mechanism of magnetic ordering. In the present study, we carried out heat capacity measurement on the MnFe-mos polycrystals to investigate its magnetic properties in detail.

2. Experimental

Polycrystalline sample of MnFe-mos was synthesized according to the method described previously [8,9]. Two types of adiabatic calorimeters were employed to carry out the heat capacity measurements according to the temperature region: 6–300 K by a low-temperature adiabatic calorimeter for small samples (microcalorimeter) [17] and 0.5–20 K by a very-low-temperature adiabatic calorimeter workable with a $^3He/^4He$ dilution refrigerator (dilution calorimeter) [18]. For the measurement with the microcalorimeter, 0.80917 g of the sample (designated as “sample A” hereafter) was loaded into a gold-plated copper cell under helium gas at 1 atm and sealed with a thin indium wire. The helium gas sealed in the cell serves as a heat exchange medium. The sample used for the dilution calorimeter was ground and pressed to ca. 1 MPa to form 1.42260 g of a pellet with 2 cm in diameter (“sample B”). This pellet was put into a gold-plated copper holder without any heat exchange media. Since remarkable disagreement between the heat capacity data for the samples A and B was found, we remeasured heat capacities by use of the microcalorimeter for 1.25044 g of the sample prepared by crashing the pellet (“sample C”). Buoyancy correction for the mass of sample was made by use of the density of $K[\{Mn(3\text{-}MeOsalen)\}_2Fe(CN)_6]\cdot 2DMF$, 1.475 g cm^{-3} [8,9].

3. Results and discussion

Molar heat capacities C_p of the MnFe-mos crystal determined for three different samples A, B, and C are plotted against temperature T in Fig. 2. The heat capacity of the virginal sample A determined by the microcalorimeter exhibited a heat capacity peak due to the antiferromagnetic phase transition at $T_N = 8.29$ K. This transition temperature agrees rather well with $T_N = 9.2$ K determined by the magnetic measurements [8,9]. Above T_N, a heat capacity tail was observed arising from the short-range-order effect of the spins which is characteristic of low-dimensional magnetic materials. The heat capacity of the pellet sample B determined by the dilution calorimeter also exhibited the antiferromagnetic phase transition and the short-range-order effect at almost the same temperatures as those of the sample A. However, the magnetic thermal anomaly slightly diminished as a whole. If one takes into account the fact that the sample B was prepared as a pellet by pressuring the powder sample A, it is very likely that this type of discrepancy found in the temperature dependence of heat capacity may be caused by a mechanochemical effect often encountered in soft materials. Below 1 K, the heat capacity showed a slight upturn which would originate from a small amount of paramagnetic impurities in the sample. In the C_p data of the pellet-crashed sample C remeasured by the microcalorimeter, the thermal anomalies were largely recovered but still smaller than those of the sample A.

To separate the magnetic heat capacities C_{mag} of these samples from the observed values, we determined the lattice heat capacity. When a magnetic phase transition occurs at low temperatures, the heat capacity far above the magnetic phase transition temperature is often approximated by the following equation:

$$C_p = c_3T^3 + c_5T^5 + c_7T^7 + c_{-2}T^{-2}, \tag{1}$$

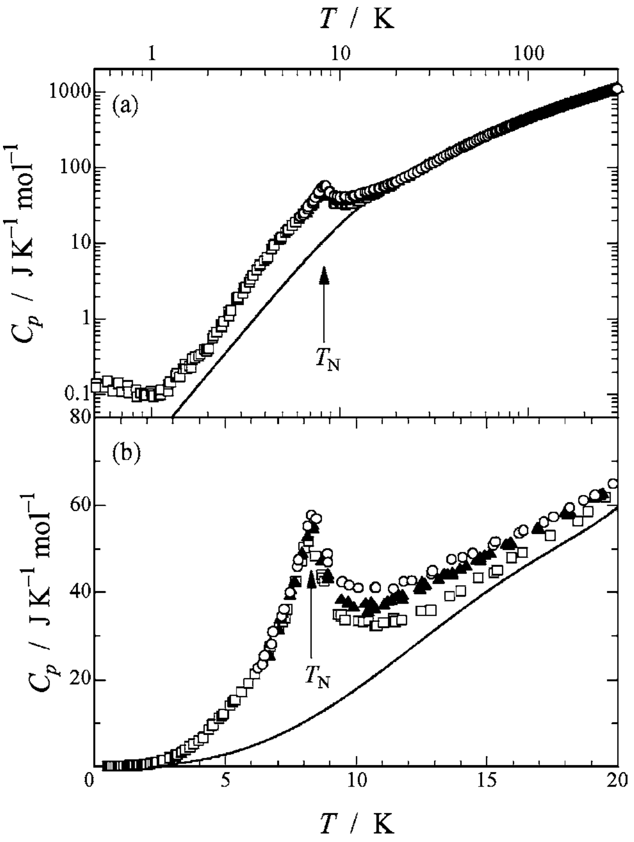

Fig. 2. Molar heat capacities of the MnFe-mos crystals: (a) in the whole experimental temperature region and (b) in the vicinity of the antiferromagnetic phase transition. (○): sample A; (□): sample B; and (▲): sample C. Solid curve indicates the lattice heat capacity for the sample A.

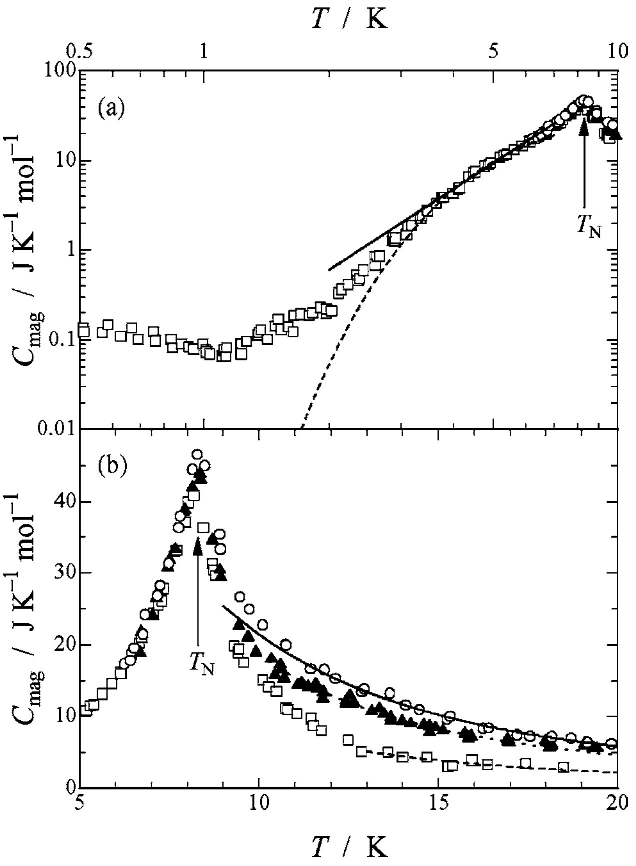

Fig. 3. Magnetic heat capacities of the MnFe-mos crystals. (○): sample A; (□): sample B; and (▲): sample C. (a) Solid curve shows the heat capacity derived from the spin wave theory for three-dimensional antiferromagnets. Dashed curve indicates the heat capacity calculated by Eq. (3). (b) Solid curve represents the theoretical heat capacity for the $S = 3/2$ two-dimensional ferromagnetic Heisenberg model of square lattice with $J/k_B = 1.6$ K. Dashed and dotted curves show the extrapolation up to infinite temperature by T^{-2} term for the samples B and C, respectively.

where the first three terms represent lattice heat capacity and the last term corresponds to a contribution from the short-range-order effect of the spin alignment [19]. We tried to fit the C_p data of the sample A alone between 12 and 20 K to Eq. (1), because the samples B and C exhibited the mechanochemical effect and thus their heat capacities were not appropriate for determination of the lattice heat capacity. On the other hand, since it seemed to be unlikely that soft grinding and pressing of the sample with as low pressure as 1 MPa would bring about a large change in the lattice vibrations, we approximated the lattice heat capacities of the samples B and C by the values for the sample A. The obtained parameters are as follows: $c_3 = 2.41 \times 10^{-2}$ J K^{-4} mol^{-1}, $c_5 = -7.02 \times 10^{-5}$ J K^{-6} mol^{-1}, $c_7 = 7.15 \times 10^{-8}$ J K^{-8} mol^{-1}, and $c_{-2} = 2.29 \times 10^3$ J K mol^{-1}.

The magnetic heat capacities for the samples A, B, and C derived by subtraction of the lattice heat capacities from the total heat capacities are plotted in Fig. 3. The heat capacity anomaly above T_N is clearly observed. This anomaly can be regarded as the short-range-order effect for the two-dimensional magnetic system from its shape and the structural analysis [8,9].

The magnetic enthalpy and entropy gains for the samples A, B, and C were evaluated by integration of the magnetic heat capacities with respect to T and ln T, respectively, where the magnetic heat capacities of the sample B at very low temperatures were commonly used as those for the samples A and C. Extrapolation down to 0 K was performed by use of Eq. (3), which is described later. On the other hand, extrapolation up to infinite temperature was done by use of the T^{-2} term in Eq. (1), where the coefficients of the T^{-2} term for the samples B and C were determined by fitting the C_{mag} data between 13 and 20 K as being 8.76×10^2 J K mol^{-1} and 1.87×10^3 J K mol^{-1}, respectively [see the dashed and dotted curves in Fig. 3(b)]. The magnetic enthalpies and entropies thus derived were $\Delta H = 373$ J mol^{-1} and $\Delta S = 31.3$ J K^{-1} mol^{-1} for the sample A, $\Delta H = 222$ J mol^{-1} and $\Delta S = 23.0$ J K^{-1} mol^{-1} for the sample B, and $\Delta H = 323$ J mol^{-1} and $\Delta S = 28.2$ J K^{-1} mol^{-1} for the sample C.

Since the MnFe-mos complex has two Mn(III) ions with $S = 2$ and one Fe(III) ion with $S = 1/2$ per formula unit, the magnetic entropy expected for such a spin system is $\Delta S = R$ ln $(5 \times 5 \times 2)$ (=32.5 J K^{-1} mol^{-1}). The experimental magnetic entropy of the sample A agrees well with the expected value. This fact suggests that the Mn(III) and Fe(III) ions in the MnFe-mos complex are in the high- and low-spin states, respectively. The experimental magnetic entropy for the sample B is extremely small in comparison with that of the sample A, whereas the entropy gain of the sample C is largely recovered. It is of interest to note here that the magnetic entropy of the sample B is rather close to the value in the case of the low-spin Mn(III), $R \ln(3 \times 3 \times 2)$ (=24.0 J K^{-1} mol^{-1}). However, it is very unlikely that such a drastic change from the high- to the low-spin state is caused by soft grinding and pressing of the sample under a low pressure such as 1 MPa. The most plausible possibility is that enhanced lattice defects and imperfections in the crystal lattice produced by the mechanochemical effect would lead to an incomplete magnetic phase transition and consequently a part of the paramagnetic species characteristic of the high-temperature phase would remain as the so-called residual paramagnetism even below the magnetic transition temperature. The former brings about a decrease of the magnetic enthalpy and entropy gained at the phase transition, while the latter would cause an additional phase transition due to the magnetic ordering of the residual paramagnetic species at extremely low temperatures as far as the third law of thermodynamics is fulfilled. In fact, the upturn of the heat capacity of the sample B encountered below 1 K [see Fig. 2(a)] seems to suggest the existence of such an additional phase transition. Such a mechanochemical effect was observed in the spin-crossover complex $[Fe^{III}(3MeOsalenEt)_2]PF_6$ [16,20–23]. Although the present complex is not a spin-crossover complex, the mechanism for the decrease of the magnetic heat capacity, enthalpy, and entropy would be quite similar to that of the spin-crossover complex.

We tried to fit the magnetic heat capacities of the sample A above T_N to two-dimensional magnetic models. As described in the introduction, the previous magnetic study [9] revealed that the present complex is a metamagnet, suggesting that the complex consists of ferromagnetic layers and the interlayer interactions are antiferromagnetic. Since the actual magnetic system of the present complex is too complicated to analyze, we approximated the actual layer by an $S = 3/2$ two-dimensional ferromagnetic Heisenberg system, where $S = 3/2$ is an averaged spin quantum number of two $S = 2$ spins and one $S = 1/2$ spin. The C_{mag} data of the sample A between 11 and 20 K was fitted to an $S = 3/2$ two-dimensional ferromagnetic Heisenberg model of square lattice [24–26]. The best fitting was obtained for the exchange interaction $J/k_B = 1.6$ K (k_B: the Boltzmann constant) as shown by a solid curve in Fig. 3(b). The derived J value is considerably small in comparison with $T_N = 8.29$ K. This might be caused by the assumption that the rather complicated actual magnetic system was approximated by a simple square lattice consisting of homogeneous spins. In some magnets among our studies, on the other hand, the J values obtained by fitting the theoretical models to the magnetic heat capacity tails above the magnetic phase transitions were smaller than the transition temperatures [27–30]. The present case shows a similar tendency.

Finally, we shall discuss about the magnetic heat capacities at very low temperatures. Heat capacities of magnetic materials at very low temperatures generally obey the spin wave theory [12]:

$$C_{mag} \propto T^{d/n}, \tag{2}$$

where d stands for the dimensionality of magnetic lattice and n is defined as the exponent in the dispersion relation: $n = 1$ for antiferromagnets and $n = 2$ for ferromagnets. Below T_N, the C_{mag} data of the sample B are proportional to T^3 (the proportional coefficient: 7.50×10^{-2} J K^{-4} mol^{-1}) in the 4.4–6 K temperature region. This suggests that the MnFe-mos crystal orders in a three-dimensional antiferromagnetic state below T_N. The estimated spin wave heat capacity is shown in Fig. 3(a) by a solid curve.

Below 4.4 K, however, the magnetic heat capacities of the sample B decreased rapidly. This suggests the existence of a large magnetic anisotropy of the Mn(III) ions, because the high spin Mn(III) ion in an octahedral ligand-field symmetry is characterized by the orbital-degenerated $^5E_{2g}$. We tried to fit the C_{mag} data of the sample B from 3 to 6 K to the following equation describing the spin wave contribution under anisotropy [31]:

$$C_{mag} = aT^{-2}e^{-(\Delta E/k_B T)}, \tag{3}$$

where ΔE stands for the energy gap between the ground and the first exited energy levels. The best fit was obtained for $a = 2.71 \times 10^4$ J K mol^{-1} and $\Delta E/k_B = 23.6$ K. The fitting result is displayed in Fig. 3(a) by a dashed curve.

As found in other metal-assembled complexes [27,28], tiny thermal anomaly observed for the present complex below 1 K is perhaps due to the presence of a small amount of imperfect ferromagnetic sheets which occurred during the sample synthesis, grinding, and pressing. This anomaly might contain the contribution due to the hyperfine interaction of the Mn nuclei [32].

4. Conclusions

Heat capacity measurements of the two-dimensional metal-assembled complex, $K[\{Mn^{III}(3\text{-}MeOsalen)\}_2Fe^{III}(CN)_6]$, were carried out in the temperature range between 0.5 and 300 K by adiabatic calorimetry. A heat capacity peak due to an antiferromagnetic phase transition was observed at $T_N = 8.29$ K, above which a large heat capacity tail due to the short-range-order effect of the spins characteristic of two-dimensional magnetic substances was found. This thermal anomaly can be expressed by the $S = 3/2$ two-dimensional ferromagnetic Heisenberg model of square lattice with $J/k_B = 1.6$ K. This fact supports that the complex possesses a two-dimensional ferromagnetic structure. The enthalpy and entropy gains due to the magnetic phase transition were $\Delta H = 373\,\mathrm{J\,mol^{-1}}$ and $\Delta S = 31.3\,\mathrm{J\,K^{-1}\,mol^{-1}}$, respectively. The value of the magnetic entropy coincides with the expected value $\Delta S = R\ln(5 \times 5 \times 2)$ (=32.5 $\mathrm{J\,K^{-1}\,mol^{-1}}$) for the spin system with two $S = 2$ spins and one $S = 1/2$ spin. Spin wave analysis of the magnetic heat capacity at low temperatures suggests that the complex is in three-dimensional antiferromagnetic state below T_N.

When the crystal of the complex was ground and pressed, the heat capacity around the magnetic phase transition was decreased. This mechanochemical effect would suppress the magnetic phase transition, leading to the decrease of the magnetic heat capacity, enthalpy, and entropy. This phenomenon was also found in the analogous complex $(\mathrm{NEt_4})[\{\mathrm{Mn^{III}(salen)}\}_2\mathrm{Fe^{III}(CN)_6}]$ [Et: ethyl, salen: *N*,*N*′-ethylenebis(salicylideneaminato) dianion]. The calorimetric results of this complex will be reported elsewhere.

Acknowledgements

This work was partially supported by a Grant-in-Aid for Scientific Research on Priority Areas “Metal-Assembled Complexes” (Area No. 401/12023229) from the Ministry of Education, Culture, Sports, Science and Technology, Japan. Chinese authors (Q.W. and Q.Y.) would like to express their deep gratitude to the Research Center for Molecular Thermodynamics for invitation, great hospitality, and scientific cooperation during their stay in Japan. Q.W. and Q.Y. also would like to thank the Ministry of Education, Culture, Sports, Science and Technology and the Japan Society for the Promotion of Science, respectively, for their financial support.

References

[1] D. Gatteschi, O. Kahn, J.S. Miller, F. Palacio (Eds.), Magnetic Molecular Materials, NATO ASI Series E, vol. 198, Kluwer Academic Publishers, Dordrecht, 1991.
[2] O. Kahn, Molecular Magnetism, Wiley-VCH, New York, 1993.
[3] O. Kahn (Ed.), Magnetism: a Supramolecular Function, NATO ASI Series C, vol. 484, Kluwer Academic Publishers, Dordrecht, 1996.
[4] E. Coronado, P. Delhaès, D. Gatteschi, J.S. Miller (Eds.), Molecular Magnetism: from Molecular Assemblies to the Devices, NATO ASI Series E, vol. 321, Kluwer Academic Publishers, Dordrecht, 1996.
[5] M.M. Turnbull, T. Sugimoto, L.K. Thompson (Eds.), Molecule-Based Magnetic Materials: Theory, Techniques, and Applications, ACS Symposium Series, vol. 644, American Chemical Society, Washington, DC, 1996.
[6] P.M. Lahti (Ed.), Magnetic Properties of Organic Materials, Marcel Dekker, New York, 1999.
[7] K. Ito, M. Kinoshita (Eds.), Molecular Magnetism: New Magnetic Materials, Kodansha & Gordon and Breach Science Publishers, Tokyo, Amsterdam, 2000.
[8] H. Miyasaka, N. Matsumoto, H. Ōkawa, N. Re, E. Gallo, C. Floriani, Angew. Chem. Int. Ed. Engl. 34 (1995) 1446.
[9] H. Miyasaka, N. Matsumoto, H. Ōkawa, N. Re, E. Gallo, C. Floriani, J. Am. Chem. Soc. 118 (1996) 981.
[10] M. Ohba, H. Ōkawa, Coord. Chem. Rev. 198 (2000) 313.
[11] A. Bhattacharjee, Y. Miyazaki, Y. Nakazawa, S. Koner, S. Iijima, M. Sorai, Phys. B 305 (2001) 56.
[12] L.J. de Jongh, A.R. Miedema, Adv. Phys. 23 (1974) 1.
[13] R.L. Carlin, Magnetochemistry, Springer-Verlag, Berlin, 1986.
[14] M. Sorai, D.N. Hendrickson, Pure Appl. Chem. 63 (1991) 1503.
[15] M. Sorai, Molecule-Based Magnetic Materials: Theory, Techniques, and Application, in: M.M. Turnbull, T. Sugimoto, L.K. Thompson (Eds.), ACS Symposium Series, vol. 644, American Chemical Society, Washington, DC, 1996, pp. 99–114.
[16] M. Sorai, Bull. Chem. Soc. Jpn. 74 (2001) 2223.
[17] Y. Kume, Y. Miyazaki, T. Matsuo, H. Suga, J. Phys. Chem. Solids 53 (1992) 1297.
[18] S. Murakawa, T. Wakamatsu, M. Nakano, M. Sorai, H. Suga, J. Chem. Thermodyn. 19 (1987) 1275.
[19] H.M.J. Blöte, Phys. B 79 (1975) 427.
[20] M.S. Haddad, W.D. Federer, M.W. Lynch, D.N. Hendrickson, J. Am. Chem. Soc. 102 (1980) 1468.
[21] M.S. Haddad, M.W. Lynch, W.D. Federer, D.N. Hendrickson, Inorg. Chem. 20 (1981) 123.
[22] M.S. Haddad, W.D. Federer, M.W. Lynch, D.N. Hendrickson, Inorg. Chem. 20 (1981) 131.
[23] M. Sorai, D.N. Hendrickson, Proceedings of the 37th Annual Meeting on Coordination Chemistry, Tokyo, 1987, p. 2B14.
[24] G.S. Rushbrooke, P.J. Wood, Mol. Phys. 1 (1958) 257.
[25] R.L. Stephenson, K. Pirnie, P.J. Wood, J. Eve, Phys. Lett. A 27 (1968) 2.
[26] K. Yamaji, J. Kondo, J. Phys. Soc. Jpn. 35 (1973) 25.
[27] K. Asano, K. Inoue, M. Nakano, Y. Miyazaki, M. Sorai, K. Nakatani, O. Kahn, Bull. Chem. Soc. Jpn. 72 (1999) 1749.
[28] K. Asano, Y. Miyazaki, W. Mori, K. Nakatani, O. Kahn, M. Sorai, Bull. Chem. Soc. Jpn. 73 (2000) 885.
[29] T. Hashiguchi, Y. Miyazaki, K. Asano, M. Nakano, M. Sorai, H. Tamaki, N. Matsumoto, H. Ōkawa, J. Chem. Phys. 119 (2003) 6856.
[30] A. Bhattacharjee, Y. Miyazaki, M. Sorai, J. Magn. Magn. Mater. 280 (2004) 1.
[31] J.A. Eisele, F. Keffer, Phys. Rev. 96 (1954) 929.
[32] Y. Miyazaki, A. Bhattacharjee, M. Nakano, K. Saito, S.M.J. Aubin, H.J. Eppley, G. Christou, D.N. Hendrickson, M. Sorai, Inorg. Chem. 40 (2001) 6632.